International Journal of Scientific Research in Mathematical and Statistical Sciences **Research Paper**
Volume-5, Issue-5, pp.01-18, October (2018) **E-ISSN:** 2348-4519

Influence of Vertical Magnetic Field on the Onset of Rayleigh-Benard-Marangoni Convection in Superposed fluid and Porous Layers with Deformable Free Surface

Ananda, K[1], Gangadharaiah, Y.H.[2*]

[1]Department of Mathematics, New Horizon College of Engineering,Bangalore-560 103, India
[2]Department of Mathematics, Sir M. Visvesvaraya Institute of Technology,Bangalore-562157, India

Available online at: www.isroset.org

Received:17/Sept/2018, Accepted:13/Oct/2018, Online: 31/Oct/2018

Abstract- When a thin horizontal fluid layer overlying a porous layer is heated from below, convection starts after that the temperature difference between the lower and upper surfaces has reached a critical value. Two effects are responsible for this motion: buoyancy and variation of the surface tension with temperature; the first effect is usually referred to as Rayleigh-Benard instability, the second as Marangoni instability. In the present work, we examine the role of the application of a vertical magnetic field on a thin horizontal electrically conducting fluid layer overlying a porous layer. An analytical solution is obtained for constant-flux thermal boundary conditions, for which the onset of supercritical cellular convection occurs at a vanishingly small wave number and can thus be predicted by the present theory. The critical Rayleigh number, R_m^c, and critical Marangoni number, M^c, are found to depend on the Chandrasekhar number, Q_m ,the depth ratio, ζ , the Darcy number, Da , the Bond number, B_0 , and the Crispation number, Cr. Results are presented for a wide range of each of the governing parameters. The results are compared with limiting cases of the problem and are found to be in agreement.

***Keywords*:** Bernard-Marangoni convection; Magnetic field; Two-layer System.

I. INTRODUCTION

The study of the electrically conducting fluid flows under the influence of a magnetic field is fundamental to many subjects, ranging from astro- and geo-physical to industrial and laboratory
scales. Diverse engineering applications, such as the design of thermonuclear fusion reactors and electromagnetic processing of materials, including semiconductor crystal growth, often rely on contactless flow control techniques by means of a magnetic field ([1]-[4]). In solidification and crystal growth processes, magnetic fields have been used to suppress fluctuations and improve the quality of products ([5]-[8]).

The flow of an electrically conducting fluid through a magnetic field generates an electromotive force, which induces electric currents. The interaction of these currents with the magnetic field creates the electromagnetic (Lorentz) body force, acting as a brake on the fluid. Owing to a complex coupling between the electromagnetic and dynamical phenomena, a wide range of magnetohydrodynamic (MHD) effects can occur within the fluid, depending on the flow's geometry, boundary conditions, and the orientation of a magnetic field and gravity. First of all, the magnetic field may change the flow characteristics by modifying its velocity profile and confining viscous effects to thin boundary layers. Furthermore, due to the stabilizing action of the Lorentz force, magnetic fields are known to accelerate the damping of perturbations.

The problem we wish to investigate is one of Rayleigh- Benard-Marangoni convection in a system consisting of porous layer underlying a fluid layer where there is magnetic field through the system. The problem of fluid flow over a porous medium is encountered in a wide range of industrial and geophysical applications, such as flows in fuel cells, filtration processes, the extraction of oil from underground reservoirs, ground-water pollution, the manufacture of composite materials, and in flow in biological materials. A detailed review is given by Nield & Bejan [9] , with current highly relevant literature including([10]-[22]).

© 2018, IJSRMSS All Rights Reserved

Nield [23] has investigated the linear stability problem of superposed fluid and porous layers with buoyancy and surface tension effects at the deformable upper free surface by using the Beavers–Joseph slip condition at the interface. The thermal stability for different systems of superposed porous and fluid regions has also been analyzed by Taslim and Narusawa [24]. Chen [25] has implemented a linear stability analysis to investigate the effect of throughflow on the onset of thermal convection in a fluid layer overlying a porous layer with an idea of understanding the control of convective instability by the adjustment of throughflow. McKay[26] has considered the onset of buoyancy-driven convection in superposed reacting fluid and porous layers. Nield [27] has argued about the modelling of Marangoni convection in a fluid saturated porous medium and has suggested the consideration of composite porous–fluid layer system in analyzing the problem. Khalili et al. [28] have obtained the closed form solution for Chen's model by considering the upper and lower boundaries are insulating to temperature perturbations.

The aim of the present study is to study analytically natural convection in a cavity consisting of a fluid layer over a saturated porous layer with magnetic field. Such problems, despite its importance in industrial and geophysical situations. In the present study we investigate the effect of magnetic field on the thermal convection of a two-layer system consists of a horizontal fluid layer overlying a layer of porous medium saturated with the same fluid with uniform heating from below (Fig. 1). The flow in porous medium is assumed to be governed by Darcy's law. Beavers-Joseph classical slip condition is used. The boundaries are considered to be insulated to temperature perturbations. A regular perturbation technique with wave number as a perturbation parameter is used to solve the eigen value problem in a closed form. The paper is organized as follows. In Sect. 2 the governing equations describing the problem are derived. Section 3 describes the analytical method used to solve the problem. The results are discussed in Sect. 4 and a conclusion is presented in Sect. 5.

II. PHYSICAL MODEL AND MATHEMATICAL FORMULATION

The composite system under investigation is shown schematically in Fig. 1. A horizontal porous layer of thickness d_m extends below a fluid layer of thickness d subject to a uniform vertical magnetic field of strength H and a uniform vertical temperature gradient. A Cartesian coordinate system (x, y, z) is chosen with the origin at the interface and the $z-$axis vertically upward. The gravity acts in the vertical direction with constant acceleration g, the lower boundary of the porous layer is taken to be rigid, while the upper surface has a deflection $\Omega(x, y, t)$ from mean (see Fig.1).

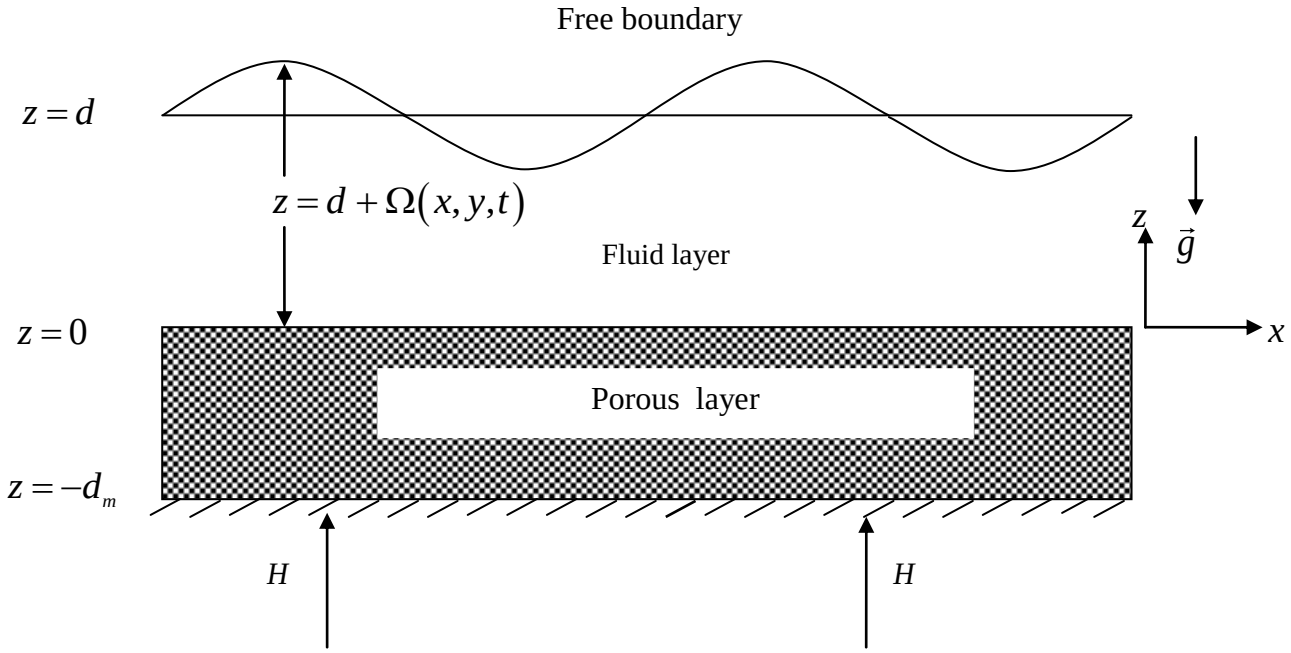

Figure 1: Physical configuration

© 2018, IJSRMSS All Rights Reserved

The governing equations for the fluid and the porous layers are:
Fluid layer:

$$\nabla \cdot \vec{V} = 0 \tag{1}$$

$$\rho_0 \left[\frac{\partial \vec{V}}{\partial t} + \left(\vec{V} \cdot \nabla\right)\vec{V} \right] = -\nabla p + \rho_0 \vec{g}\left[1 - \alpha\left(T - T_0\right)\right] + \mu \nabla^2 \vec{V} + \frac{\mu}{4\pi}\left(\vec{H} \cdot \nabla\right)\vec{H} \tag{2}$$

$$\frac{\partial T}{\partial t} + \left(\vec{V} \cdot \nabla\right)T = \kappa \nabla^2 T \tag{3}$$

$$\frac{\partial \vec{H}}{\partial t} = \left(\vec{H} \cdot \nabla\right)\vec{V} - \left(\vec{V} \cdot \nabla\right)\vec{H} + \eta \nabla^2 \vec{H} \tag{4}$$

Porous layer:

$$\nabla \cdot \vec{V}_m = 0 \tag{5}$$

$$\frac{\rho_0}{\phi}\frac{\partial \vec{V}_m}{\partial t} = -\nabla p_m - \frac{\mu_m}{K}\vec{V}_m + \rho_0 \vec{g}\left[1 - \alpha\left(T_m - T_0\right)\right] + \frac{\mu_m}{4\pi}\left(\overrightarrow{H_m} \cdot \nabla\right)\overrightarrow{H_m} \tag{6}$$

$$A\frac{\partial T_m}{\partial t} + \left(\vec{V}_m \cdot \nabla_m\right)T_m = \kappa_m \nabla^2 T_m . \tag{7}$$

$$\frac{\partial \overrightarrow{H_m}}{\partial t} = \left(\overrightarrow{H_m} \cdot \nabla\right)\vec{V} - \left(\overrightarrow{V_m} \cdot \nabla\right)\overrightarrow{H_m} + \eta_m \nabla^2 \overrightarrow{H_m} \tag{8}$$

In the above equations, $\vec{V} = (u, v, w)$ is the velocity vector, p is the pressure, T is the temperature, , H is the magnetic field, and κ is the thermal diffusivity, μ is the fluid viscosity, η magnetic permeability, α is the thermal expansion coefficient, ϕ is the porosity of the porous medium, A is the ratio of heat capacities and ρ_0 is the reference fluid density, The subscript m refers to the value of the parameter in the porous region.

2.1 The Boundary conditions

Suppose that $z = d$ and $z = -d_m$ are maintained at constant temperature T_u and T_l respectively. In terms of W and W_m, the axial velocity components of the fluid and porous layers , these requirements lead to the following conditions

$$W = 0, \frac{\partial T}{\partial z} = 0, \frac{\partial H}{\partial z} = 0 \qquad at \quad z = d \tag{9}$$

$$W_m = 0, \frac{\partial T_m}{\partial z} = 0, \frac{\partial H_m}{\partial z} = 0 \qquad at \quad z = -d_m \tag{10}$$

At the deformable free surface, $z = d + \Omega(x, y, t)$, $|\Omega| << 1$

$$\frac{\partial \Omega}{\partial t} + u\frac{\partial \Omega}{\partial x} + v\frac{\partial \Omega}{\partial y} = w, \qquad k_t \nabla T.\hat{n} + GT = 0 \tag{11}$$

$$2\mu d_{nt} = \frac{\partial \sigma}{\partial T}\nabla T.\hat{t}, \qquad p_a - p + 2\mu d_{nn} = \sigma \nabla.\hat{n}. \tag{12}$$

© 2018, IJSRMSS All Rights Reserved

$$\left.\begin{aligned} & W = W_m,\ T = T_m \\ & \kappa \frac{\partial T}{\partial z} = \kappa_m \frac{\partial T_m}{\partial z},\ p_m = p - 2\mu \frac{\partial w}{\partial z} \\ & \frac{\partial H}{\partial z} = \frac{\partial H_m}{\partial z} = 0 \end{aligned}\right\} \quad at \quad z = 0 \tag{13}$$

and the final condition is due to Beavers & Joseph [30] which has the form

$$\frac{\partial u}{\partial z} = \frac{\beta}{\sqrt{K}}\left(u - u_m\right),\ \frac{\partial v}{\partial z} = \frac{\beta}{\sqrt{K}}\left(v - v_m\right) \quad at \quad z = 0 \tag{14}$$

The basic state is quiescent and is of the form

$$\vec{V} = 0,\ \vec{V_m} = 0, \vec{H} = \left(0,0,h\right),\ \vec{H}_m = \left(0,0,h_m\right) \tag{15}$$

The temperature distributions in the basic state are given by

$$T_b\left(z\right) = T_0 - \frac{\left(T_0 - T_u\right)z}{d}, \qquad 0 \le z \le d \tag{16}$$

$$T_{mb}\left(z_m\right) = T_0 - \frac{\left(T_l - T_0\right)z_m}{d_m}, \qquad -d_m \le z_m \le 0 \tag{17}$$

Where $T_0 = \dfrac{\kappa d_m T_u + d\kappa_m T_l}{\kappa d_m + \kappa_m d}$ is the interface temperature.

To investigate the stability of the basic state, infinitesimal disturbances are superimposed in the form

$$\vec{V} = \vec{V}',\ T = T_b\left(z\right) + \theta,\ p = p_b(z) + p',\ \vec{V}_m = \vec{V}_m',\ \vec{H} = H\left(z\right) + \psi,\ \vec{H}_m = H_m\left(z\right) + \psi_m \tag{18}$$

$$T_m = T_{mb}\left(z_m\right) + \theta_m,\quad p_m = p_{mb}(z_m) + p_m'. \tag{19}$$

Following the standard linear stability analysis procedure and noting that the principle of exchange of stability holds, we arrive at the following stability equations:

$$\left(D^2 - a^2\right)^2 W - QD^2 W = Ra^2\Theta \tag{20}$$

$$\left(D^2 - a^2\right)\Theta = -W \tag{21}$$

$$\left(D^2 - a^2\right)\psi = -DW \tag{22}$$

$$\left(D_m^2 - a_m^2\right)W_m + Da\ Q_m D_m^2 W_m = -R_m a_m^2 \Theta_m \tag{23}$$

$$\left(D_m^2 - a_m^2\right)\Theta_m = -W_m. \tag{24}$$

$$\left(D_m^2 - a_m^2\right)\psi_m = -D_m W_m \tag{25}$$

Here, W is the amplitude of perturbed vertical velocity and Θ is the amplitude of perturbed temperature, ψ is the amplitude of perturbed magnetic field, $D = d/dz$, $R = \alpha g\left(T_0 - T_u\right)d^3/\nu\kappa$ is the Rayleigh number, $a = \sqrt{l^2 + m^2}$ is the overall horizontal wave number and $\nabla^2 = \nabla_h^2 + \partial^2/\partial z^2$ is the Laplacian operator with $\nabla_h^2 = \partial^2/\partial x^2 + \partial^2/\partial y^2$. The corresponding quantities for the porous region are W_m, Θ_m, ψ_m $D_m = d/dz_m$, $R_m = \alpha g\left(T_l - T_0\right)d_m K_v/\nu\kappa_{mv} = RDa\zeta^{-4}\varepsilon_T^2, Q_m = \zeta^2 Q$, $a_m = \sqrt{\tilde{l}^2 + \tilde{m}^2}$ and $\nabla_m^2 = \nabla_{mh}^2 + \partial^2/\partial z_m^2$ with

© 2018, IJSRMSS All Rights Reserved

$\nabla_{mh}^2 = \partial^2/\partial x_m^2 + \partial^2/\partial y_m^2$. Further, $Da = K_v/d_m^2$ is the Darcy number, $\varepsilon_T = \kappa/\kappa_m$ is the ratio of thermal diffusivities.

The boundary conditions are:

$$W = D\Theta + B_i(\Theta - Z) = D\psi = 0 \quad \text{at } z = 1 \tag{26}$$

$$D^2W + Ma^2(\Theta - Z) = 0 \quad \text{at } z = 1 \tag{27}$$

$$-Cr\left(D^2 - 3a^2 - Q\right)DW + \left(B_0 + a^2\right)a^2 Z = 0 \quad \text{at } z = 1 \tag{28}$$

$$W_m = D_m\Theta_m = D_m\psi_m = 0 \quad \text{at } z_m = -1. \tag{29}$$

At the interface (i.e., z = 0) the continuity of velocity, temperature, heat flux, normal stress and the Beavers and Joseph 1967 slip conditions are imposed. Accordingly, the conditions are:

$$W = \frac{\zeta}{\varepsilon_T}W_m, \Theta = \frac{\varepsilon_T}{\zeta}\Theta_m, \; D\Theta = D_m\Theta_m \tag{30}$$

$$D\psi = 0 = D_m\psi_m \tag{31}$$

$$\left[D^2 - 3a^2\right]DW = \frac{-\zeta^4}{\varepsilon_T Da}D_m W_m \tag{32}$$

$$\left[D^2 - \frac{\beta\zeta}{\sqrt{Da}}D\right]W = \frac{-\beta\zeta^3}{\varepsilon_T\sqrt{Da}}D_m W_m \tag{33}$$

where $\zeta = d/d_m$ is the ratio of fluid layer to porous layer thickness and β is the Beavers-Joseph slip parameter. Thus, the problem is reduced to an eigen value problem consisting of a eighth order ordinary differential equation in the fluid layer and a sixth order ordinary differential equation in the porous layer, subject to 14 boundary conditions. If matching of the solutions in the two layers is to be possible, the wave numbers must be the same for the fluid and porous layers, so that we have $a/d = a_m/d_m$ and hence $\zeta = a/a_m$.

III. SOLUTION BY REGULAR PERTURBATION TECHNIQUE

Since the critical wave number is exceedingly small for the assumed temperature boundary conditions ([9]), the eigen value problem is solved using a regular perturbation technique with wave number a as a perturbation parameter. Accordingly, the dependent variables are expanded in powers of a^2 in the form

$$(W, \Theta, \psi) = \sum_{i=0}^{N}\left(a^2\right)^i (W_i, \Theta_i, \psi_i) \tag{34}$$

$$(W_m, \Theta_m, \psi_m) = \sum_{i=0}^{N}\left(\frac{a^2}{\zeta^2}\right)^i (W_{mi}, \Theta_{mi}, \psi_{mi}) \tag{35}$$

Substitution of Eqs. (34) and (35) into Eqs. (20)–(25) and the boundary conditions (26)–(33) yields a sequence of equations for the unknown functions $W_i(z), \Theta_i(z), \psi_i(z), W_{mi}(z_m)$ and $\Theta_{mi}(z_m), \psi_{mi}(z)$ for $i = 0,1,2,3.....$.

At the leading order in a^2 Eqs. (20)–(25) become, respectively,

$$D^4W_0 - QD^3W_0 = 0 \tag{36}$$

$$D^2\Theta_0 = W_0 \tag{37}$$

$$D^2\psi_0 = -DW_0 \tag{38}$$

$$D_m^2 W_{m0} + Q_m D^2 W_{m0} = -R_m \tag{39}$$

© 2018, IJSRMSS All Rights Reserved

$$D_m^2\Theta_{m0} = -W_{m0} \tag{40}$$

$$D_m^2\psi_{m0} = -DW_{m0} \tag{41}$$

and the boundary conditions $(26)-(33)$ become

$$W_0 = 0, \quad D\Theta_0 = 0, \; D\psi_0 = 0, \quad D^3W_0 - Q\,DW_0 = 0 \qquad \text{at} \quad z = 1 \tag{42}$$

$$W_{m0} = 0, \quad D_m\Theta_{m0} = 0, \qquad \text{at} \quad z_m = -1. \tag{43}$$

And at the interface($i.e\ z = 0$)

$$W_0 = \frac{\zeta}{\varepsilon_T}W_{m0}, \; \Theta_0 = \frac{\varepsilon_T}{\zeta}\Theta_{m0}, \; D\Theta_0 = D_m\Theta_{m0}, D\psi_0 = 0 = D_m\psi_{m0} \tag{44}$$

$$D^3W_0 - D^2W_0 = \frac{-\zeta^4}{Da\xi\varepsilon_T}D_mW_{m0} \tag{45}$$

$$D^2W_0 - \frac{\beta\zeta}{\sqrt{Da\xi}}DW_0 = \frac{-\beta\zeta^3}{\varepsilon_T\sqrt{Da\xi}}D_mW_{m0}. \tag{46}$$

The solution to the zeroth order Eqs. $(36)-(41)$ is given by

$$W_0 = 0, \quad \Theta_0 = \frac{\varepsilon_T}{\zeta}, \psi_0 = 1, \; W_{n0} = 0, \; \psi_{m0} = 1, \Theta_{m0} = 1. \tag{47}$$

At the first order in a^2 Eqs. $(20)-(25)$ then reduce to

$$D^4W_1 - QD^2W_1 = R\frac{\varepsilon_T}{\zeta} \tag{48}$$

$$D^2\Theta_1 - \frac{\varepsilon_T}{\zeta} = -W_1 \tag{49}$$

$$D^2\psi_1 - 1 = -DW_1 \tag{50}$$

$$D_m^2W_{m1} + Da\,Q_mD_m^2W_{m1} = -R_m \tag{51}$$

$$D_m^2\Theta_{m1} - 1 = W_{m1} \tag{52}$$

$$D^2\psi_{m1} - 1 = -DW_{m1} \tag{53}$$

and the boundary conditions $(26)-(33)$ become

$$W_1 = 0, \quad D\Theta_1 = 0, \; D^2W_1 + M\left(\frac{\varepsilon_T}{\zeta} - Z_0\right) = D^3W_1 - QDW_1 - \frac{B_0}{Cr}Z_0 = 0 \quad at \quad z = 1 \tag{54}$$

$$W_{m1} = 0, \quad D_m\Theta_{m1} = 0, \qquad at \quad z_m = -1. \tag{55}$$

And at the interface($i.e\ z = 0$)

$$W_1 = \frac{1}{\zeta\varepsilon_T}W_{m1}, \; \Theta_1 = \frac{\varepsilon_T}{\zeta^3}\Theta_{m1}, \quad D\Theta_1 = \frac{1}{\zeta^2}D_m\Theta_{m1}, D\psi_1 = 0 = D_m\psi_{m1} \tag{56}$$

$$D^3W_1 - \eta D^2W_1 = \frac{-\zeta^2}{Da\xi\varepsilon_T}D_mW_{m1} \tag{57}$$

$$D^2W_1 - \frac{\beta\zeta}{\sqrt{Da\xi}}DW_1 = \frac{-\beta\zeta}{\varepsilon_T\sqrt{Da\xi}}D_mW_{m1}. \tag{58}$$

The general solutions of Eq. (49) and (52) are respectively given by

© 2018, IJSRMSS All Rights Reserved

$$W_1 = R\left[C_1 + C_2 z + C_3 e^{-\sqrt{Q}z} + C_4 e^{-\sqrt{Q}z} - \frac{\varepsilon_T}{2Q\zeta} z^2 \right] \tag{59}$$

$$W_{m1} = R\left[C_5 z_m + C_6 - \frac{Da\,\varepsilon_T{}^2}{2\zeta^4 \left(1 + Da\,Q_m\right)} z_m^2 \right] \tag{60}$$

where

$$C_1 = \left(\frac{C_2}{\varepsilon_T B_0 Q} - C_4 \right),\ C_2 = \left(\frac{\varepsilon_T}{\zeta} - \frac{C_1}{2\Delta} - C_3 - e^Q C_4 \right),\ C_3 = \frac{\left(b_{10} + b_9 C_6\right)}{b_4},\ C_4 = \frac{\left(b_6 \varepsilon_T \zeta - \varepsilon_T \zeta C_3 + C_3\right)}{\Delta C_1}$$

$$C_5 = \frac{C_1}{2\zeta(1+2\Delta)} + C_6, C_6 = \frac{\beta\zeta^3\left(\sqrt{DaQ} - Q_m\right)}{2\zeta(1+2\Delta)},\ b_1 = \left(\frac{2\zeta^2\sqrt{Da}}{2Q\Delta} + Q_m\zeta^3 \right) b_2 = \left(\zeta^2\sqrt{DaQ} - \beta\zeta^3 \right)$$

$$b_3 = \left(\Delta_2\sqrt{DaQ_m} - \frac{\beta\zeta^3}{\varepsilon_T\zeta} \right),\ b_4 = \left(\frac{\varepsilon_T Q}{6\eta\zeta} - \frac{\beta\zeta^3\sqrt{Q_m}}{\varepsilon_T\zeta} \right), b_5 = \left(Q-1\right)Q + \sqrt{DaQ_m},\ b_6 = \left(\frac{2\varepsilon_T}{6\eta\zeta} - \frac{\sqrt{DaQ_m}}{\varepsilon_T\zeta} \right),$$

$$b_7 = \left(b_1 b_3 - \frac{b_2}{\varepsilon_T\zeta} \right),\ b_8 = \left(b_3 b_5 - \frac{b_2}{\varepsilon_T\zeta} \right),\ b_9 = \left(b_4 b_5 + 2 b_7 b_6 \right), b_{10} = \frac{\left(b_1 b_7 - b_8 b_6\right)}{\left(b_1 b_7 - \frac{b_4}{\varepsilon_T\zeta} \right)},$$

$$\Delta = 6\ \zeta^2\sqrt{\mathrm{Da}\xi}(\mathrm{B}_0\text{-Cr M}) + (2\ \mathrm{B}_0 - 3\ \mathrm{CrM})\zeta^3\beta + 6\mathrm{B}_0\mathrm{Da}\xi\beta\ (1\text{-}\zeta)$$

Equations (48) and (51) involving $D^2\Theta_1$ and $D_m^2\Theta_{m1}$ respectively provide the solvability requirement which is given by

$$\int_0^1 W_1\, dz + \frac{1}{\zeta^2}\int_{-1}^0 W_{m1}\, dz = \frac{\varepsilon_T}{\zeta} + \frac{1}{\zeta^2} \tag{61}$$

The expressions for W_1 and W_{m1} are back substituted into Eq. (61) and integrated to yield an expression for the critical Rayleigh number R_m^c, which is given by

$$R_m^c = \frac{\left(\frac{\varepsilon_T}{\zeta} + \frac{1}{\zeta^2} \right)\left(\frac{Da\,\varepsilon_T^2}{\zeta^4} \right)}{\left(\Delta_1 C_1 + \Delta_2 C_2 + \Delta_3 C_3 + \Delta_4 C_4 \right) + \frac{1}{\zeta^2}\left(-C_5 + \Delta_4 C_6 + \Delta_5 \right)} \tag{63}$$

Where

$$\Delta_1 = \left(6Cr\zeta\eta - DaQ\varepsilon_T MQ\right) + \zeta^3\left(144Cr + \zeta\varepsilon_T 6\mathrm{B}_0 + 144Cr/\zeta^3 + 72B_0 Q_m M\varepsilon_T\left(\varepsilon_T + \zeta\right)/\zeta^3\right)$$

$$\Delta_2 = Q_m + \beta\zeta M\varepsilon_T\zeta^4\left(72Cr + B_0 + B_0 Da\left(36\varepsilon_T + 48\zeta\right)/\zeta^4\right)$$

$$\Delta_3 = \left[\frac{\left(6Cr\zeta - DaQ\varepsilon_T M\right)}{3Q} + \frac{\left(Q + 2Q_m\right)}{\left(1 - e^{Q_m}\right)}\left(\frac{e^{Q_m}}{Q_m} - \frac{4e^{Q_m}}{DaQ\varepsilon_T M} + \frac{8\left(1-Q_m\right)}{Q^3} \right) \right]$$

$$\Delta_4 = \left[\frac{2Q}{\beta\varepsilon_T} + \frac{\left(Q + DaQ\varepsilon_T M\right)}{\left(1 - e^{Q_m}\right)}\frac{\left(e^Q - 1\right)}{\left(Q_m + \beta\varepsilon_T\right)} + \frac{3+Q}{Q_m} + \frac{\left(Q + DaQ\varepsilon_T MQ_m\right)}{\left(1 - 2e^{Q_m}\right)} + \frac{2e^{-Q_m}}{Q_m^2} + \frac{2\left(e^{-Q_m} - 1\right)}{Q_m^3} \right].$$

© 2018, IJSRMSS All Rights Reserved

$$\Delta_5 = \left[\frac{2QQ_m^3}{\beta\varepsilon_T} + \frac{\left(QQ_m^2 M\right)}{\left(1-e^{Q_m}\right)} \frac{\left(Q_m^2 e^Q - 1\right)}{\left(Q_m - 3\beta\varepsilon_T Q_m^3\right)} + \frac{2\left(e^{-Q_m} - Q_m^2\right)}{Q_m^3} \right]$$

The expression for R_m^c is evaluated for different values of various physical parameters and the results are discussed in detail in the next section.

IV. RESULT AND DISCUSSION

We consider a linear stability analysis to investigate analytically the effects of deformable surface and magnetic field on the onset of Rayleigh-Benard -Marangoni convection in a system consisting of porous layer underlying a fluid layer heated from below. The marginal stability of the composite system considered in this investigation is given by equation (63). We can check this formula against known results for the following limiting cases:

(i) Case of a pure porous layer ($\zeta << 1$) :

In the absence of Magnetic field (Chandrasekhar number $Q = 0$), it is readily found from equation (63) that

$$R^c = 12, \tag{64}$$

In agreement with the result predicted in the past by Nield [30], for the case of a horizontal Darcy porous layer heated from the bottom by a constant heat flux.

(ii) Case of a horizontal fluid layer ($\zeta >> 1$) :

In the absence of Magnetic field (Chandrasekhar number $Q = 0$), it is readily found from equation (63) that

a) $R^c = 320$ (65)

which is also a value reported in the past by Sparrow et al. [31] in the case of a fluid layer with a solid horizontal lower boundary and a free upper surface.

b) $R^c = 720$ (66)

which is also a value reported in the past by Sparrow et al.[31] in the case of a fluid layer with a rigid boundaries.

(iii) Case of a horizontal fluid layer ($\zeta >> 1$) for pure Marangoni Convection.

In the absence of Magnetic field (Chandrasekhar number $Q = 0$) and absence of surface deflection $(Cr = 0)$, it is readily found from equation (63) that

$$M^c = 48, \tag{67}$$

is the known exact value for a signal fluid layer ([32]). The critical Marangoni number computed for different values of Q when ε_T = 0.725, Da = 0.001, β = 1 and Cr = 0 are tabulated in Table 1. The results of Wilson [33] are also exhibited in the Table for the sake of comparison. It is seen that our results are in good agreement with those of Wilson [33] for pure Marangoni convection in a signal fluid layer.

To gain physical insight into the onset of the convection, we illustrate the eigen functions of vertical velocity W and corresponding streamline patterns in Figures 2. Figures 2a–c present the analytically predicted velocity profile at the vertical

© 2018, IJSRMSS All Rights Reserved

centerline of a system for $\zeta = 1$ and various values of the Chandrasekhar number Q_m. A significant change in the velocity field is observed upon varying the values of Da and Q_m. When the permeability of the porous medium is low enough, for instance Q_m for $Da = 10^{-4}$ (when the permeability of the porous medium is low) Figures 1a-c indicates that the intensity of the convective motion inside the system is relatively weak. In fact, the major part of the flow is confined in the pure fluid layer $(0 \le z \le 1)$, while the fluid is almost at rest in the porous part. Figure 2d shows some part of the flow in porous layer $(-1 \le z \le 0)$ when the permeability of the porous medium is high ($Da = 0.1$).

Table 1: Comparison of critical Marangoni number with those of Wilson [33] for different values of Q $(\zeta \to \infty$ and $Cr = 0)$ when Da =0.001, ε_T = 0.725, β = 1.

Q	Wilson [33] M^c	Present study $(\zeta \to \infty$ and $Cr = 0)$ M^c
10^{-4}	48.00024	48.0135
10^{-3}	48.00240	48.0147
10^{-2}	48.02400	48.17821
10^{-1}	48.24000	48.3678
1	50.39997	50.83241
10	71.97468	72.13891

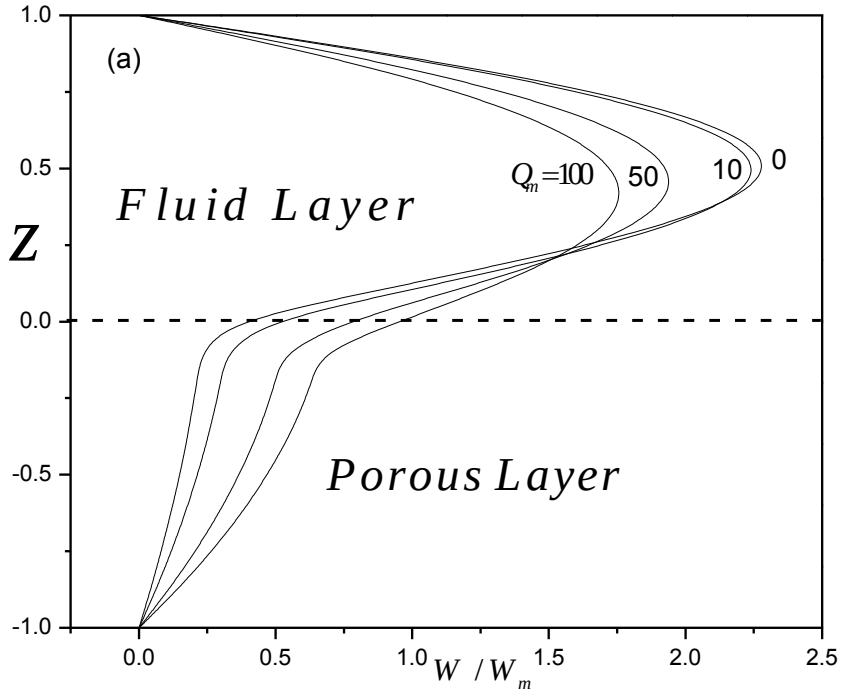

© 2018, IJSRMSS All Rights Reserved

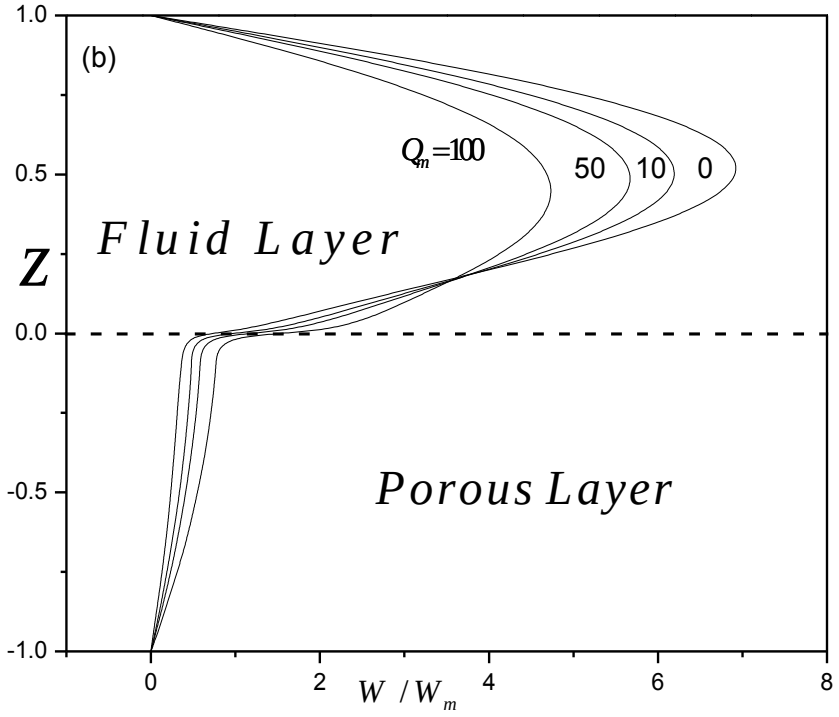

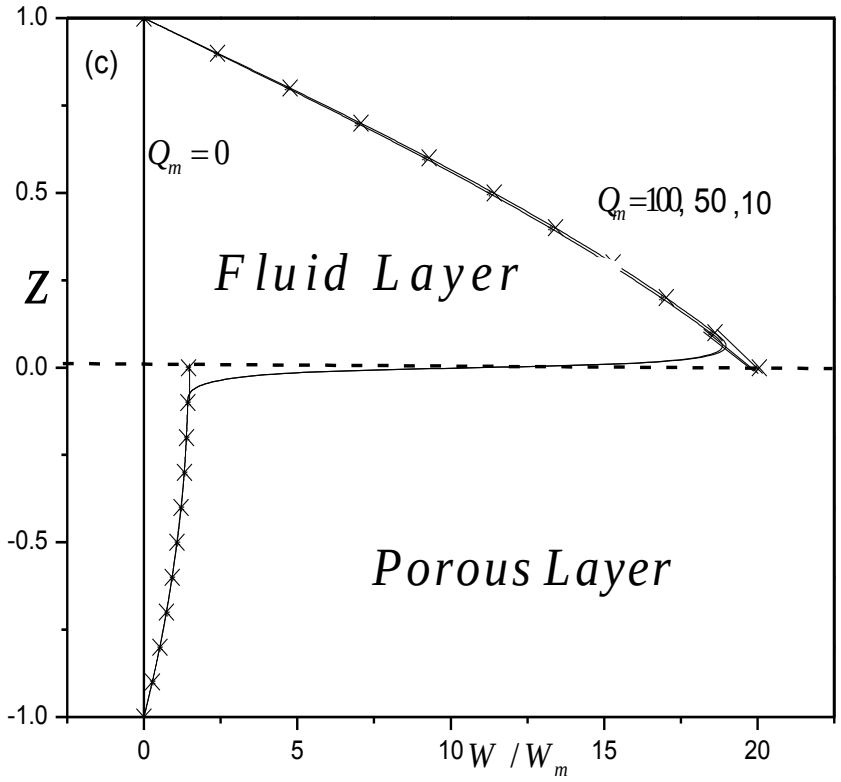

© 2018, IJSRMSS All Rights Reserved

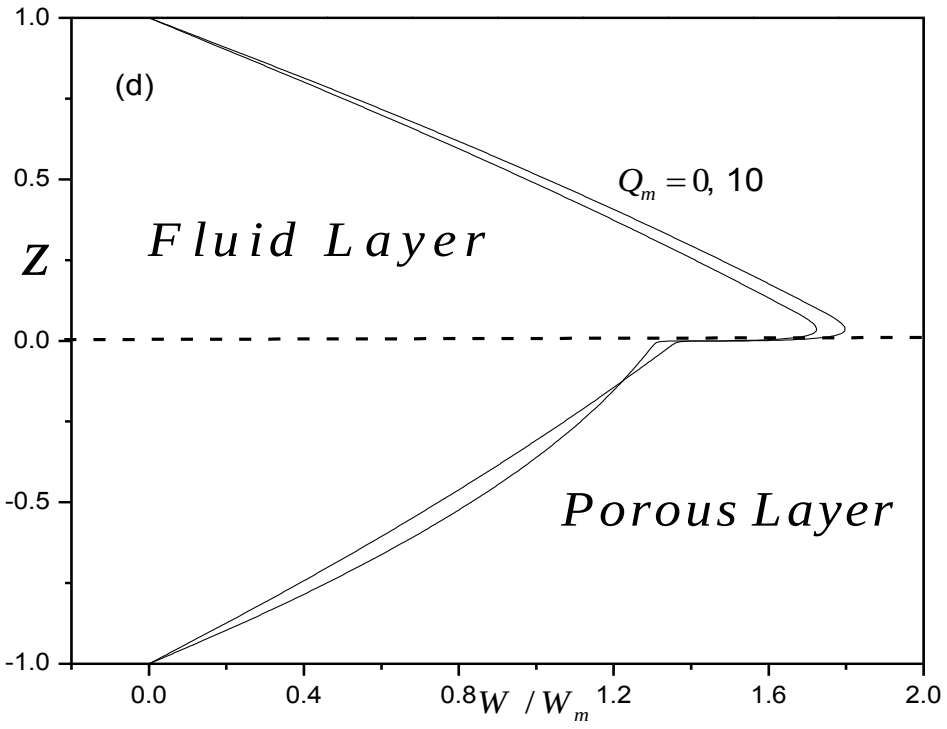

Figure 2 : The effect of Q_m , for a fluid–porous bed system, on the vertical velocity distribution

(**a**) $\zeta = 1,\ Da = 10^4$ (**a**) $\zeta = 0.5,\ Da = 10^4$ (**a**) $\zeta = 0.1,\ Da = 10^4$ (**a**) $\zeta = 1,\ Da = 0.1.$

First we will discuss Rayleigh-Benard convection (in the absence of Marangoni number $M = 0$) and the results are presented for The results are presented for $\sqrt{Da} = 3.04 \times 10^{-3}$ (which correspond to 3-cm-deep porous layer consisting of 3-mm-diameter glass beads ([25]) $B_o = 0.1,\ \varepsilon_T = 0.725, \beta = 1$ *and* $Cr = 0$ the range of depth ratio $\zeta = 10^{-4}$ approximating pure porous layer case to $\zeta = 1$ (two layers of equal depth). The variation of R_m^c obtained as a function of depth ratio ζ for different values of the Chandrasekhar number Q_m are presented in a Figure.3. Figure 3 reveals the effect ζ on the values of R_m^c for various values of Q_m . It is clear from this figure that there is a precipitation drop of the values of the critical R_m^c as ζ increases, which means that the magnetic field has a stabilizing effect in this system. The variation of R_m^c obtained as a function of Chandrasekhar number Q_m for different values of the depth ratio ζ are presented in a Figure.4. It is clear from the figure that R_m^c increases continuously as Q_m increases which means that the magnetic field has a stabilizing effect in this system. Moreover R_m^c decreases continuously as the thickness of the fluid layer increases

© 2018, IJSRMSS All Rights Reserved

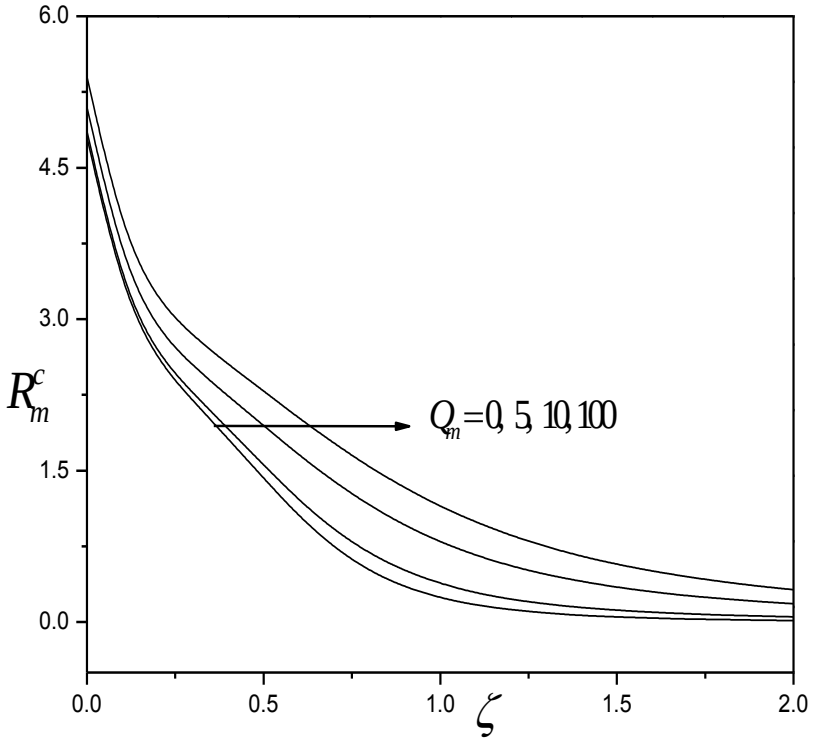

Figure 3 : Critical Rayleigh number R_m^c versus ζ for different values of Q_m .

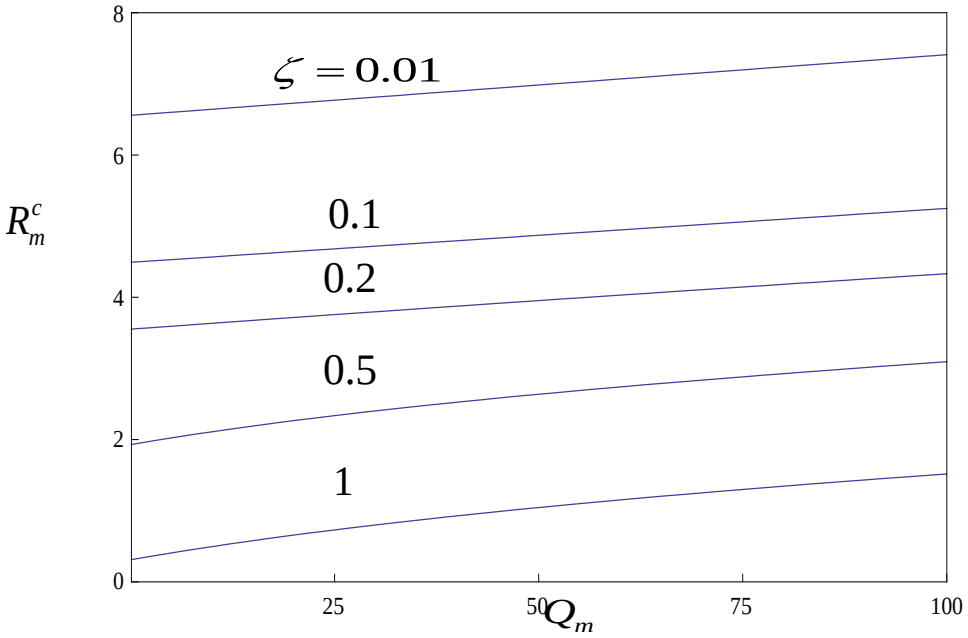

Figure 4 : Critical Rayleigh number R_m^c versus Q_m for different values of ζ .

© 2018, IJSRMSS All Rights Reserved

In the absence of thermal buoyancy $(i.e\ R=0)$ we merely consider the Marangoni convective instability at the upper free surface. The effects of Cr on M^c are shown in Figure 5 and 6. Figure 6 represents the graph of M^c as a function of Q_m for different values of Cr (i.e., influence of surface tension) for fixed values of $Da=4\times10^{-6}, B_o=0.1,$ $\varepsilon_T=0.725, \beta=1, \zeta=1, R=0,\quad B_i=0$ (Since we are dealing with layers of small thickness, the value of B_i does not appreciably affect the results for $B_i=0$, Takashima[34]. From figure, it may be noted that an increase in value of Q_m is to decrease the value of M_c and thus making system more unstable. The reason being that an increase in Cr is to increase the deflection of the upper free surface, which in turn, promotes instability much faster. But this trend goes on diminishing with an increase in the value of Q_m value of $Cr=0.1$, M_c remains almost invariant with Q_m .

The variation of M_c obtained as a function of depth ratio ζ for different values of Bond number B_0 for fixed values of $Da=4\times10^{-6}, B_i=0, \varepsilon_T=0.725.\ , \beta=1, Cr=10^{-4}$ *and* $Q_m=10.$ are presented in a figure8. From figure8 it is obvious that in contrast to the effect of $Cr,$ increase in the value of B_0 makes the system more stable, although it has negligible effect for small values of ζ. the reason for this may be attributed to the fact that an increase in the gravity effect, which keep the free surface flat against the effect of surface tension, which forms a meniscus on the free surface, and hence an increase in B_0 makes the system more stable.

Figure 9 show the effect of varying β on M_c as a function of depth ratio ζ . We note that virtually all values of β > 1 have no effect on onset of convection. When fluid layer is relatively thin, however, an increase in β from 0.1 to 1 slightly increases the critical Marangoni number. But a reverse behaviour is noticed with further increase in the thickness of the fluid layer and ultimately all the curves of β merge in to one for values of $\zeta>0.3$.

The variation of M^c obtained as a function of depth ratio ζ for different values of Q_m and Da when $\varepsilon_T=0.725, \beta=1, Cr=0.001, B_0=0.1,$ are presented in a Fig9 . As expected, the effect of decrease in Da is to increase the critical Marangoni number. Furthermore, the variation in Da has a significant effect on the onset of convection for the values of $\zeta\le0.2,$ while the curves of different Da merge in to one when $\zeta>0.2$ for both types of temperature conditions. Further it indicates that the presence of magnetic field is to hasten delay the onset of Marangoni convection.

The main results are summarized on fig. 11 where the critical Marangoni M_c is represented as a function of the critical Rayleigh number R_m^c for various values of Chandrasekhar number Q_m. For a given value of Q_m, all the representative points below the curve denote stable situations while the points which are found beyond the curve represent unstable motions.

© 2018, IJSRMSS All Rights Reserved

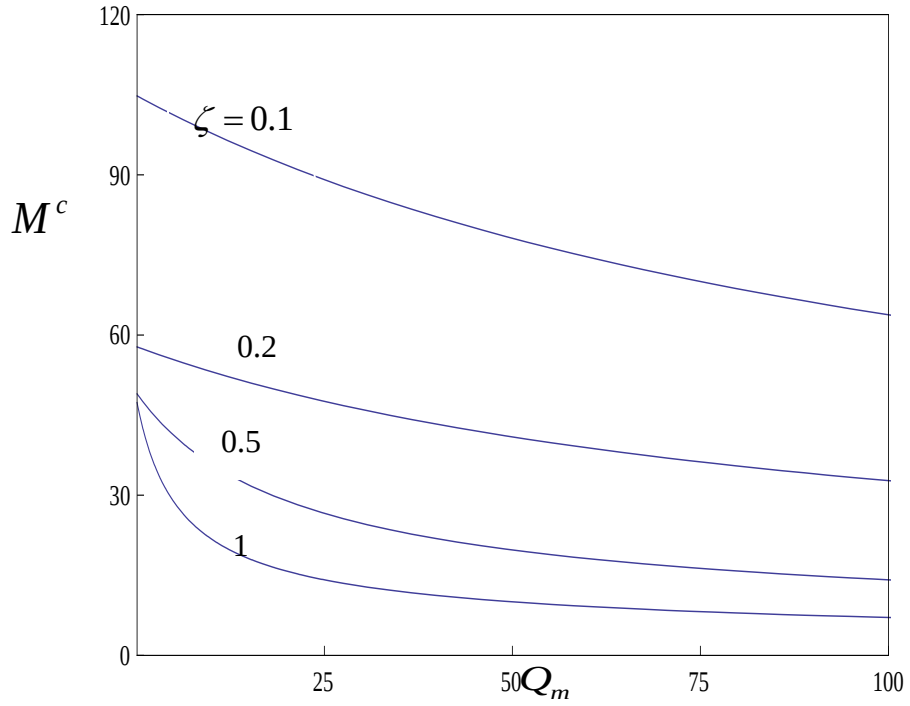

Figure 5 : Critical Marangoni number M^c versus Q_m for different values of ζ with $Cr = 0.001$.

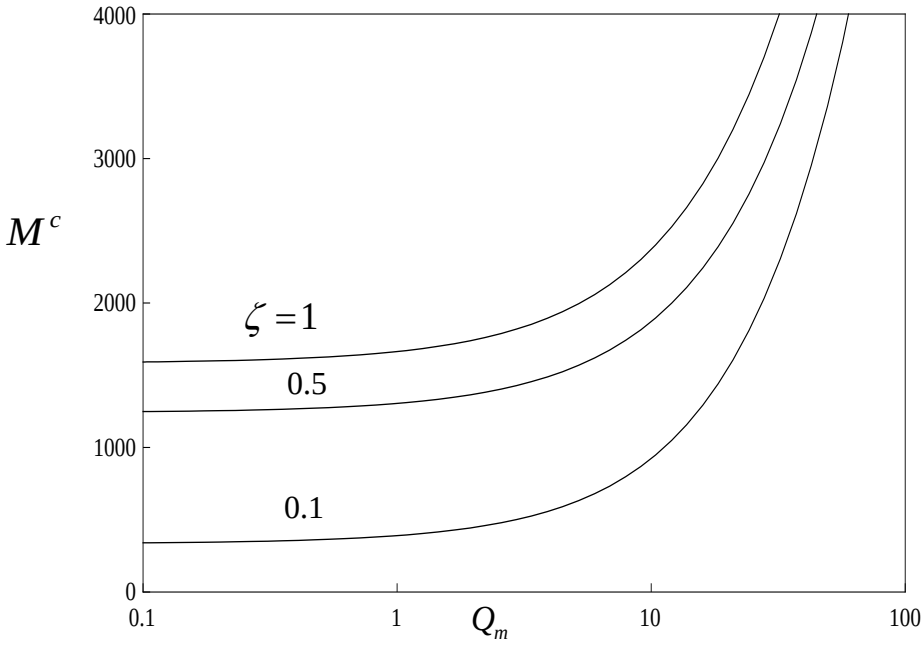

Figure 5 : Critical Marangoni number M^c versus Q_m for different values of ζ with $Cr = 0$.

.

© 2018, IJSRMSS All Rights Reserved

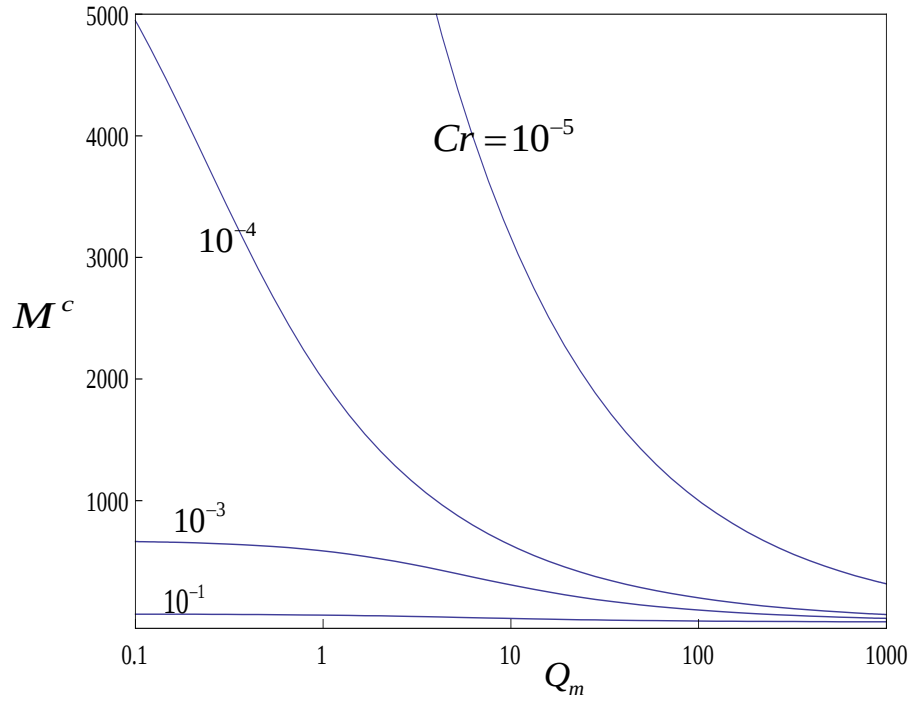

Figure 6 : Variations of the critical Marangoni number M^c and depth ratio ζ with different values of Cr ($Q_m = 10, Da = 4\times10^{-6}, \varepsilon_T = 0.725,\ B_o = 0.1, R = 0$ *and* $\beta = 0.5$).

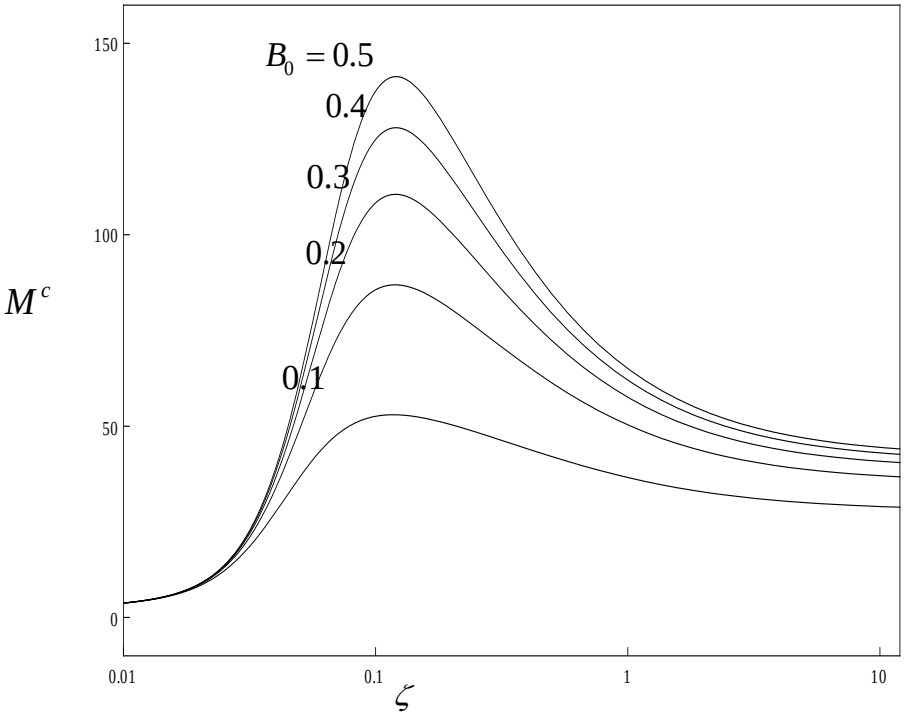

Fig. 8. Variation of M^c with ζ for different values of B_0 when $\xi = 0.5 = \eta$, $\varepsilon_T = 0.725$ $Da = 4\times10^{-6}, Cr = 0.001. R = 0$ *and* $\beta = 1.$

© 2018, IJSRMSS All Rights Reserved

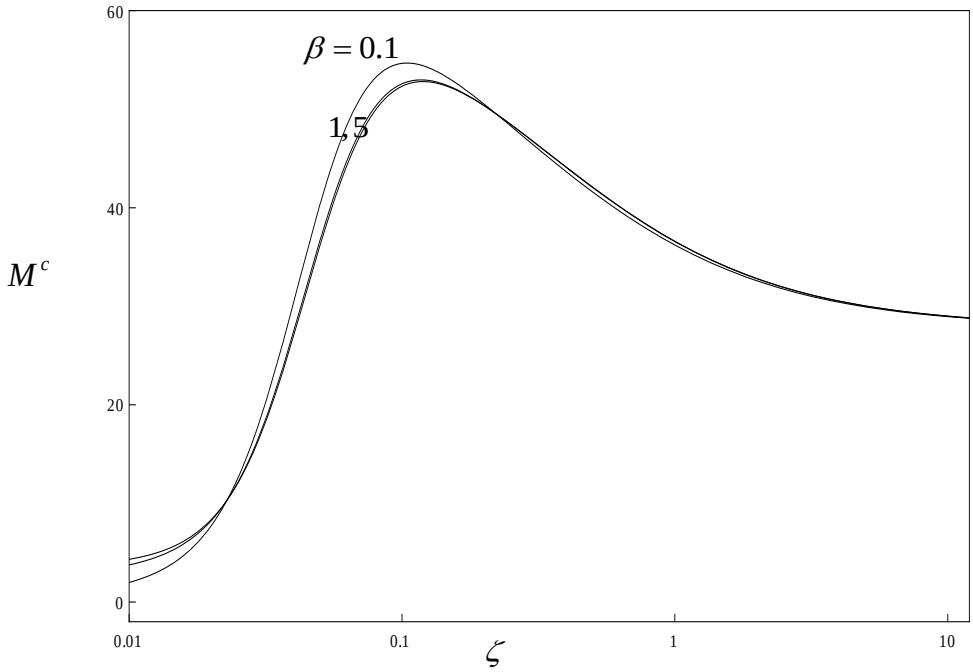

Fig. 9. Variation of M^c with ζ for different values of β when, $\varepsilon_T = 0.725$ $Da = 4\times10^{-6}, B_o = 0.1, R = 0$ *and* $Cr = 0.001.$

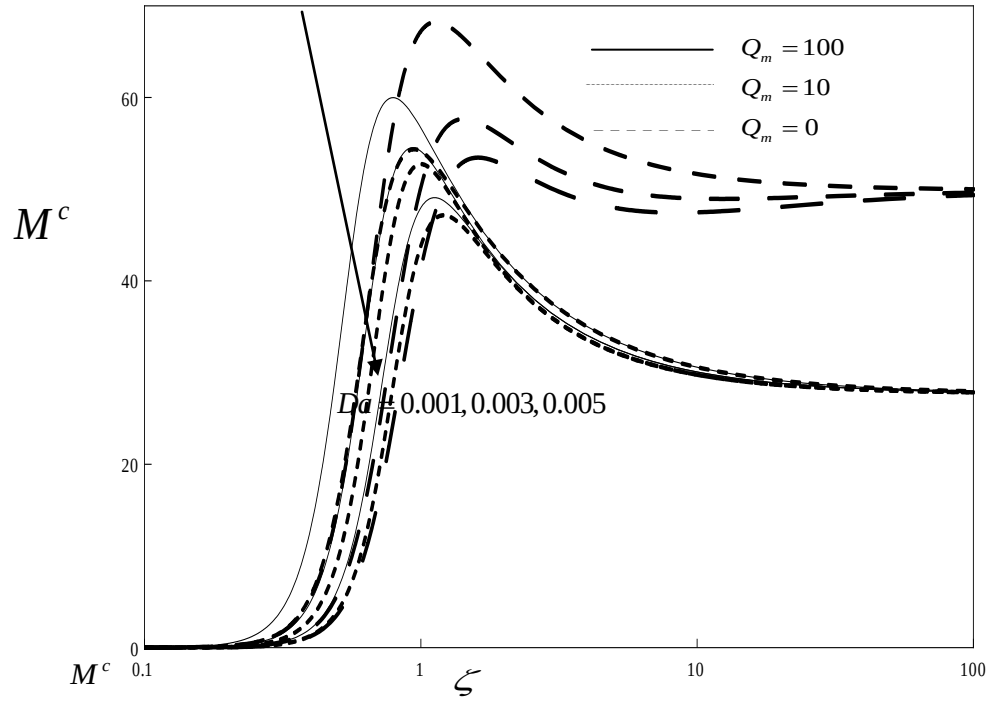

Figure 10 : Variations of the critical Marangoni number M^c and depth ratio ζ with different values of Darcy number Da and Chandrasekhar number Q_m.

© 2018, IJSRMSS All Rights Reserved

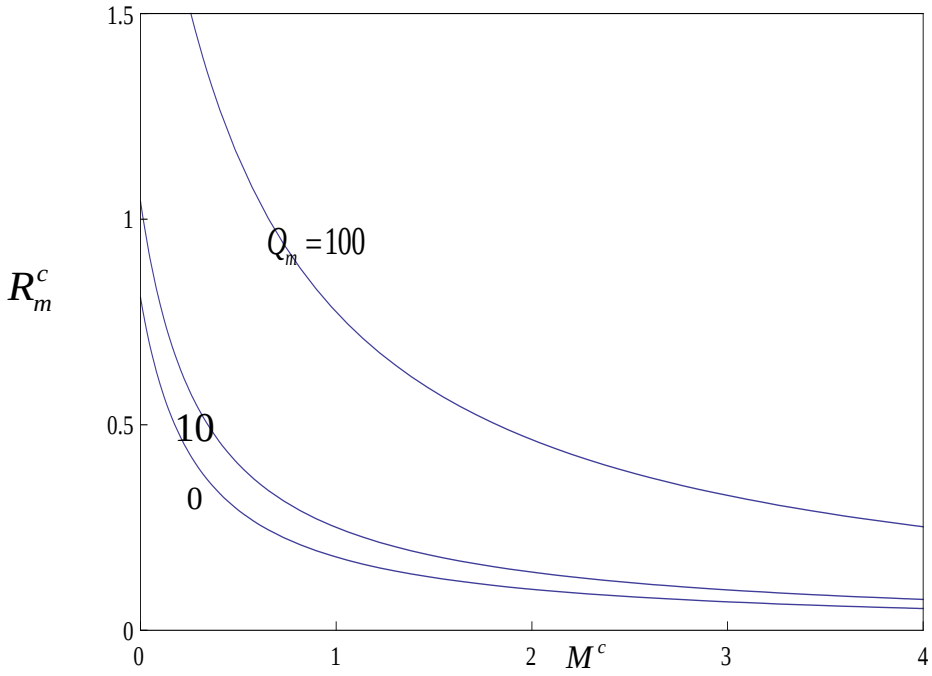

Fig.11 Critical Rayleigh number R_m^c versus M^c for different values of Q_m .

V. CONCLUSSION

The above analysis was concerned with a linear analysis of Benard-Marangoni instability in an electrically conducting fluid layer overlying a porous layer, heated from below and submitted to a vertical magnetic field with deformable upper free surface. If the free surface is non deformable $(Cr = 0)$ then the presence of the magnetic field (Q_m) always has the stabilizing effect of increasing the R_m^c / M^c, and any particular disturbance can be stabilized completely by a sufficiently strong magnetic field (Q_m). If the free surface is allowed to deform $(Cr \neq 0)$ The effect of allowing the free surface to deform $(Cr \neq 0)$ is always to destabilize the system.We conclude that a vertical magnetic field always has a stabilizing effect on the onset of steady Benard-Marangoni convection in superposed fluid and porous layers, but that when the free surface is deformable situations with a sufficiently large Marangoni number M^c will always have unstable modes no matter how strong the applied magnetic field.

REFERENCES

[1] S. Molokov, R. Moreau, H. Moffatt. (2007). Magnetohydrodynamics: Historical Evolution and Trends. *Springer*.
[2] H. Fredriksson, U. and Akerlind (2012). Solidification and Crystallization Processing in Metals and Alloys. *J. Wiley & Sons*.
[3] M. Braunsfurth, A., Skeldon , A., Juel, T. Mullin, D. Riley (1997). Free convection in liquid gallium. *J. Fluid Mech.* 342, 295–314.
[4] M. Sheikholeslami (2017).Numerical simulation of magnetic nanofluid natural convection in porous media. *Phys. Lett. A.* 381 (5) 494–503.
[5] D. Hurle (1993). Crystal Pulling from the Melt, *Springer*.
[6] G. Dhanaraj, K. Byrappa, V. Prasad, and M. Dudley (2010). Springer Handbook of Crystal Growth, *Springer*.
[7] T. Alboussiere, A. Neubrand, J. Garandet, R. and Moreau (1997). Segregation during horizontal Bridgman growth under an axial magnetic field. *J. Cryst. Growth* 181, 133–144.
[8] H. Ozoe (2005). Magnetic Convection. Imperial College Press.
[9] Nield, D.A, and Bejan, A (2006). Convection in Porous Media. Third. ed. Springer-Verlag. New York.
[10] Straughan, B. (2002). Sharp global nonlinear stability for temperature-dependent viscosity convection. Proc. R. Soc. Lond. A. 458, 1773–1782.
[11] Straughan, B. (2008). Stability and wave motion in porous media. *Appl. Math. Sci. Series, vol. 165.New York, NY: Springer.*
[12] Carr, M.(2004). Penetrative convection in a superposed porous- medium–fluid layer via internal heating, *J. Fluid Mech*. 509, 305–329.

© 2018, IJSRMSS All Rights Reserved

[13] Chang, M. H. (2004). Stability of convection induced by selective absorption of radiation in a fluid overlying a porous layer, *Phys. Fluids.* 16, 3690–3698.
[14] Chang, M. H. (2005). Thermal convection in superposed fluid and porous layers subjected to a horizontal plane couette flow, *Phys. Fluids.* 17, 064106-1–064106-7.
[15] Chang, M. H. (2006). Thermal convection in superposed fluid and porous layers subjected to a plane Poiseuille flow, *Phys. Fluids*. 18, 035104-1–035104-10.
[16] Shivakumara, I. S., Suma, S. P., Indira, R., and Gangadharaiah, Y. H. ,(2012). Effect of internal heat generation on the onset of Marangoni convection in a fluid layer overlying a layer of an anisotropic porous medium. *Transp. Porous Med*. Vol.92, pp.727-743.
[17] GangadharaiahY.H.(2013). Double-Diffusive Marangoni convection in a composite system. *International Journal of Innovative Research in Science, Engineering and Technology*.131, 137-144.
[18] Suma, S. P., Gangadharaiah, Y. H, Shivakumara, I. S., and Indira, R. (2012). Throughflow effects on penetrative convection in superposed fluid and porous layers, *Transp. Porous Med.* Vol.93, pp 1107-1127.
[19] Gangadharaiah,Y.H (2016) . Bernard-Marangoni Convection in a Fluid layer Overlying a Layer of an Anisotropic Porous Layer with Deformable Free surface. ***J**ournal of **A**pplied **F**luid **M**echanics*. 9, 221-229.
[20] Gangadharaiah,Y.H(2017) . Onset of Benard–Marangoni Convection in a Composite Layers with Anisotropic Porous Material. ***J**ournal of **A**pplied **F**luid **M**echanic*s. 10, 661-666.
[21] Gangadharaiah,Y.H.(2017). Onset of Darcy–Benard Penetrative Convection in Porous Media . ***J**ournal of **A**pplied **F**luid **M**echanics*. 10, 661-666.
[22] Hill, A. A, and Straughan, B. (2009). Poiseuille flow in a fluid overlying a highly porous material, *Adv. Water Resour*. 32, 1609-1614.
[23] Nield, D. A. (1977). Onset of convection in a fluid layer overlying a layer of a porous medium, *J. Fluid Mech.* 81, 513–522.
[24] Taslim, M. E., and Narusawa, V. (1989). Thermal stability of horizontally superposed porous and fluid layer. *ASME J. Heat Transf.* 111, 357-362.
[25] Chen, F. (1990). Throughflow effects on convective instability in superposed fluid and porous layers, *J. Fluid. Mech*. 231, 113–133.
[26] McKay, G. (1998). Onset of buoyancy-driven convection in superposed reacting fluid and porous Layers, *J. Engg. Math.* 33, 31–46.
[27] Nield, D.A. (1998). Modelling the effect of surface tension on the onset of natural convection in a saturated porous medium, *Transport Porous Med.* 31, 365–368.
[28] Khalili, A., Shivakumara., I.S, and Suma, S.P. (2003). Convective instability in superposed fluid and porous layers with vertical throughflow. *Transp. Porous Med*. 51, 1–18.
[29] Beavers, G.S., and Joseph, D.D. (1967). Boundary conditions at a naturally permeable wall.*J. Fluid Mech.* 30, 197–207.
[30] Nield, D.A. (1987). Throughflow effects on the Rayleigh-Benard convective instability problem. *J. Fluid Mech.* 185, 353–360.
[31] Sparrow, E.M., Goldstin, R.J., and Jonssn, V.K.(1964). Thermal instability in horizontal fluid layer: effect of boundary conditions and non-linear temperature. *J. Fluid Mech.* 18, 513–529.
[32] Pearson. J. R. A. (1958). On convection cells induced by surface tension. *J. Fluid Mech.* 4,489–500.
[33] Wilson, S. K. (1994). The effect of uniform magnetic field on the onset of steady Marangoni convection in layer of conducting fluid with a prescribed heat flux at its lower boundary. *Physics of fluid.* 6, 3591.
[34] Takashima, M.(1981). Surface tension driven instability in a horizontal liquid layer with a deformable free surface. I. Stationary convection, *Journal of the Physical Society of Japan.* 50, 2745–2750.

About the Author

Mr.Ananda.K, obtained his M.Sc., from Bangalore University, Bangalore and M.Phil., from Sri Venkateswara University, Tirupati. He has been teaching Engineering Mathematics for undergraduate students for the past 11 years. He has published/ presented more than 10 research papers in national and international journals/ conferences and his research area of interest are fluid mechanics: convection: stability analysis.

Dr.Gangadharaiah.Y.H, obtained his M Sc from Bangalore University, Bangalore and Ph.D from Visvesvarya Technological University, Belgaum. He has teaching Engineering Mathematics for undergraduate and post graduate students for past several years. He has published/ presented more than 30 research papers in national and international journals/ conferences and his research area of interest are fluid mechanics: convection: stability analysis.

© 2018, IJSRMSS All Rights Reserved